RICHARD S. HIRSH

A NUMERICAL SIMULATION OF VORTEX MOTION IN A STRATIFIED ENVIRONMENT AND COMPARISON WITH EXPERIMENTS

A most distinctive feature characterizing the oceanic environment is ambient density stratification resulting from temperature and salinity. Fluid motions in that stratified background are markedly different from their counterparts in unstratified flow. A classic problem in fluid mechanics is the motion of a pair of counterrotating vortices, such as those shed from a wing tip. Stratification adds enough complications to the problem so that in the early 1970s a controversy arose about the vortex behavior in those circumstances. With the advent of digital computers, the ability to solve numerically the governing equations of fluid motion allowed the investigation of previously intractable nonlinear problems such as vortex motion. To demonstrate aspects of stratified fluid dynamic behavior, a computational study has been made of some simple phenomena associated with vortex motion.

INTRODUCTION

The inclusion in an incompressible fluid, of a density variation resulting from perturbations about a stably stratified background density profile, leads to a wide variety of phenomena that have no parallel in unstratified flows. The additional degree of freedom provided by the ability to excite potential energy (because of the displacement of fluid particles from their neutrally buoyant positions) provides the source for such diverse phenomena as internal wave coupling with turbulent motion and wake collapse behind slender bodies. The extension of Kelvin's theorem to allow for the production of new vorticity arising from stratification effects influences the dynamic phenomena of the interaction of wing-trailing vortex pairs.

The subject of wake collapse has been surveyed from the experimental point of view by Lin and Pao,[1] and examples of predictive capabilities are shown in Hassid.[2] The coupling of the random nondeterministic part of the wake flowfield was covered experimentally in a recent paper by Gilreath and Brandt[3] and from a numerical standpoint by Hirsh and Stuhmiller[4] and by Metcalfe and Riley.[5] The present study will concentrate only on the wake flow produced by the trailing vortex system of a wing, the so-called "vortex wake." The main emphasis will be on the numerical prediction of various phenomena of vortex wakes, including only as much physics in the equations to be solved as is necessary to predict the desired phenomena; e.g., the turbulent aspects of the flow will be neglected but commented on when necessary. The predictions will be compared with extant experiments and with new tests performed at APL.

Two vastly different phenomena associated with the flow past a wing in a stratified medium are examined numerically and compared with experimental results. The parameter that characterizes each problem is a vortex Froude number, F_V, the ratio of vortex inertia to buoyancy. For low Froude numbers, calculations demonstrate that a linear inviscid description of the flow is possible; for $F_V \approx 1$, the full nonlinear equations are necessary, but the inviscid approximation still predicts the gross features of the flow. When F_V is larger than 1.5, it is obvious that turbulence will have to be accounted for. The computed solutions are produced by a specially constructed numerical procedure that conserves energy even in the $F_V \approx 1$ regime when there is nonlinear transfer between kinetic and potential energy.

EQUATIONS OF THE PROBLEM

For the two sets of tests to be predicted in this work, the focus of attention was on the nondissipative phenomena (i.e., the generation of internal waves or the suppression of vortex motion) that occurred because of the inclusion of stratification. Thus, in selecting what terms had to be used to describe the flow, only the nonlinear terms and additional stratification terms in the usual equations of motion were considered. No molecular viscosity or turbulence model was used; the equations are inviscid. The consequences of this decision will be noted whenever necessary. It will also be assumed that the generated vortices were shed by a wing moving rapidly in the x direction. It can be shown that if the wing Froude number, F_W, is large, the motion can be considered as an unsteady two-dimensional phenomenon in the y-z plane.

Under those conditions, the equations of inviscid, incompressible, stratified flow are the Euler equations modified by the Boussinesq approximation, the incompressibility condition, and the evolution equation for the density. In two dimensions, with z vertical and y horizontal, these appear as

$$\rho_0 \left(\frac{\partial v}{\partial t} + v \frac{\partial v}{\partial y} + w \frac{\partial v}{\partial z} \right) = - \frac{\partial p}{\partial y} ; \quad (1a)$$

$$\rho_0 \left(\frac{\partial w}{\partial t} + v \frac{\partial w}{\partial y} + w \frac{\partial w}{\partial z} \right) = - \frac{\partial p}{\partial z} - \rho' g ; \quad (1b)$$

$$\frac{\partial v}{\partial y} + \frac{\partial w}{\partial z} = 0 \text{ ; and} \quad (2)$$

$$\frac{\partial \rho'}{\partial t} + v \frac{\partial \rho'}{\partial y} + w \frac{\partial \rho'}{\partial z} = - w \frac{d\bar{\rho}}{dz} , \quad (3)$$

where v and w are the horizontal and vertical velocities, p is the fluid pressure, and g is the acceleration of gravity. The fluid density is

$$\rho = \rho_0 + \bar{\rho}(z) + \rho'(y,z,t) ,$$

where ρ_0 is a constant, $\bar{\rho}$ represents the static background stratification, and ρ' is the perturbation from the rest case caused by the motion. Usually, in the ocean, $\rho_0 \gg \bar{\rho} \gg \rho'$.

For computational purposes, it is sometimes easier to eliminate the pressure from Eqs. 1 and form the vorticity of the fluid (ζ = curl **v**). This gives, in place of 1,

$$\frac{\partial \zeta}{\partial t} + v \frac{\partial \zeta}{\partial y} + w \frac{\partial \zeta}{\partial z} = \frac{g}{\rho_0} \frac{\partial \rho'}{\partial y} . \quad (4)$$

Equation 4 shows the extension to Kelvin's theorem whereby a density perturbation in a stratified fluid acts as a source of vorticity that would not otherwise be present.

In order to gain insight into the nature of the possible solutions to these equations, it is convenient to cast them into nondimensional form, scaling each variable by a quantity characteristic of its expected magnitude. In our particular instance, there are two distinct time scales over which a significant aspect of the fluid motion can take place. There is the dynamic time scale, which is the time a characteristic length would be traversed by a fluid particle traveling at the characteristic velocity, and there is the buoyant time scale based on the natural buoyancy frequency of the stratified flow, the Brunt-Väisälä frequency, N, defined by

$$N^2(z) = - \frac{g}{\rho_0} \frac{d\bar{\rho}}{dz} . \quad (5)$$

Each of the scalings gives a slightly different form of the nondimensional governing equations.

For the dynamic scaling, Eqs. 3 and 4 become, respectively,

$$\frac{\partial \zeta}{\partial t} + v \frac{\partial \zeta}{\partial y} + w \frac{\partial \zeta}{\partial z} = \frac{1}{F_V^2} \frac{\partial \rho'}{\partial y} , \quad (6a)$$

$$\frac{\partial \rho'}{\partial t} + v \frac{\partial \rho'}{\partial y} + w \frac{\partial \rho'}{\partial z} = n^2 w , \quad (7a)$$

where all quantities are now dimensionless and n^2 is the dimensionless Brunt-Väisälä frequency. If the buoyant scaling is used, the equations become

$$\frac{\partial \zeta}{\partial t} + F_V \left(v \frac{\partial \zeta}{\partial y} + w \frac{\partial \zeta}{\partial z} \right) = \frac{\partial \rho'}{\partial y} , \quad (6b)$$

$$\frac{\partial \rho'}{\partial t} + F_V \left(v \frac{\partial \rho'}{\partial y} + w \frac{\partial \rho'}{\partial z} \right) = n^2 w . \quad (7b)$$

F_V is defined as

$$F_V = \frac{U_c}{N_c L_c} , \quad (8)$$

where U_c, N_c, and L_c are the characteristic scales for velocity, the Brunt-Väisälä frequency, and length used to make Eqs. 6 and 7 dimensionless.

Equations 6a and 7a are valid when $F_V \gg 1$, i.e., when the buoyancy has very little influence on the nonlinear dynamics of the motion. Conversely, Eqs. 6b and 7b are valid when $F_V \ll 1$ and buoyancy dominates the flow. When F_V approaches zero, the equations that result from 6b and 7b describe the propagation of linear internal waves.

From this discussion on scaling, three distinct regimes are obvious. One is the large Froude number regime where the density perturbation acts, to lowest order, as a passive scalar advected by the velocity field. This regime is effectively that of classic flows and is the subject of the now-standard field of computational fluid dynamics. It will not be dealt with further. The other regimes (low Froude numbers and $F \approx 1$) will be covered by the experiments cited and the numerical methods and predictions given. The $F = 0$ limit is the realm of much linearized analysis for wave motion, but the full nonlinear equations will be used to determine if the scaling produces linear results. The $F \approx 1$ regime is of interest because it is there that all the terms in the equation are necessary and the nonlinear advective terms and buoyancy terms are of equal order.

METHOD OF SOLUTION

The nonlinear, coupled, partial differential equations 6 and 7 were solved numerically on the VAX 11/780 computer to determine whether some experimental results could be predicted as inviscid phenomena. The absence of actual dissipation within the governing differential equations was used as a guide in selecting the finite difference procedure to integrate the equations. Methods were sought that would eliminate or minimize any artificial dissipation introduced by the numerics. A seldom-used time integration procedure was coupled to a modified standard spatial discretization in a computer code called FISHBONE (for FInite-difference or Spectral Hydrocode for BOussinesq Nonlinear Equations) to produce the numerical results. Details of the numerical method can be found in Ref. 6.

One measure of the accuracy of FISHBONE results can be gauged from its energy conservation properties. For a constant N fluid, Eqs. 6 and 7 can be shown to imply that the total (nondimensional) energy contained in the fluid,

$$E = \frac{1}{2}\left(v^2 + w^2 + \frac{1}{F_V{}^2}\,\rho'^2\right),$$

is constant. Results obtained from FISHBONE calculations showed that the computed sum of the kinetic and potential energies was indeed constant.

The equations to be solved require both initial and boundary conditions. Because the simulations were to be of experiments run in towing tanks, the boundary conditions imposed for the normal velocities were simply no flow through the boundaries of the finite difference grid over which the numerical integration took place, and free-slip boundary conditions for the tangential velocities. For the initial conditions, since the counterrotating vortices were produced by the passage of a towed wing and since the equation for the vorticity (Eq. 6) was to be solved, a simple aerodynamic formula of Thwaites[7] was used to predict the strength of the shed vortices based on the wing speed and angle of attack. The distance between these tip vortices, denoted by b, was taken to be $(\pi/4)$ times the wing span, as was also given by classic aerodynamic theory. The only parameter that was at all adjustable concerned the assumed distribution of the vorticity because point vortices cannot be computed by the methods used in FISHBONE. The vorticity was assumed to be distributed in a region surrounding the $\pi/4$ point according to

$$\zeta = \frac{\Gamma}{2\pi r_0{}^2}\exp\left[-(y^2 + z^2)/2r_0{}^2\right],$$

and r_0 was adjusted so that the discrete values of the vorticity at the finite-difference grid points could be integrated to give the total wing circulation, Γ, within 1 percent of the Thwaites value.

Since the vortex motion and the internal waves resulting from that motion were the focus of this numerical investigation, no trailing turbulent wake was included to account for the passage of the vortex-generating wing, nor was any density perturbation assumed on the initial plane. Thus, once the speed and span of the wing were given, the computations could proceed.

EXPERIMENTAL CONFIGURATION

Two series of experiments were performed in the APL Hydrodynamics Laboratory towing tank. An extensive description of the experimental facility may be found in an article by Brandt and Hurdis.[8]

The experiments were performed by first stratifying the water in the tank to a preset Brunt-Väisälä profile. The two sets of experiments consisted of measurements in a constant Brunt-Väisälä profile and in a variable profile. Once the background Brunt-Väisälä profile was established, a rectangular, symmetrical airfoil wing was towed through the tank at a preset speed and angle of attack. A high-speed strut containing 19 measuring probes spaced 1 centimeter apart vertically was then shot across the wake of the wing, triggered by a laser timing system. The probes measured conductivity, which was converted to density perturbations by means of a pretest calibration. The data were then converted to fluid displacement values and displayed on raster plots (see Fig. 1, for example). The entire data-taking procedure is automated on a PDP-11 computer so that the raster plots appear automatically after each experimental run. Each run produced a raster plot of the wake at a specific time after the passage of the wing. The output of all the experiments was a time history of the evolution of the vortex wake.

In addition to the APL experiments, two other investigations have been reported[9,10] that were directed more toward the gross features of the vortex motion (they were performed at higher values of F_V) than toward a detailed description of the density field. They determined the time history of the position of the vortex center and, in particular, the maximum height to which the vortex rises in the stratified fluid. Normally, with no stratification, the vortices would move unimpeded, but the presence of stratification limits that motion.

All of the foregoing experiments were used to test the predictive capabilities of the FISHBONE computer code.

COMPARISON OF PREDICTIONS WITH EXPERIMENTS

The conditions of the tests run at APL were such that F_V in Eqs. 6 and 7 was approximately 1/35. Following the arguments describing the equations, this means that the resulting motion is described by a set of linear equations. There is no motion of the vortex pair, and

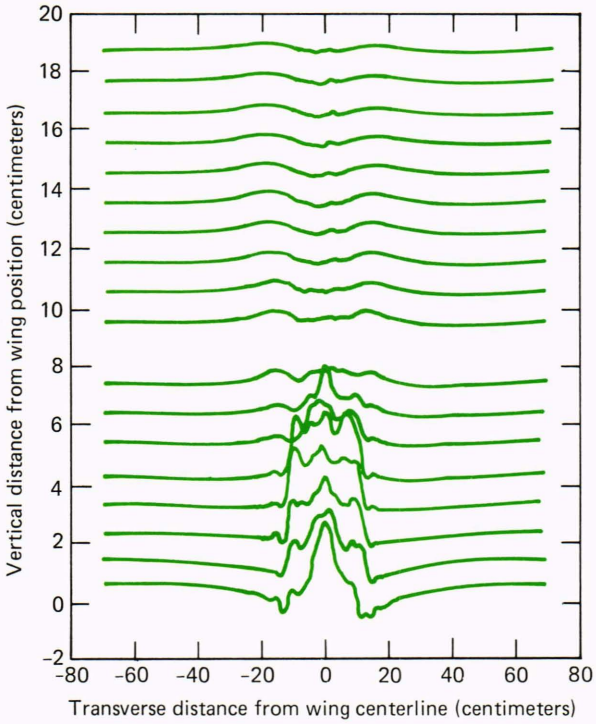

Figure 1—Measured displacements for constant N case; t = 0.5 Brunt-Väisälä (BV) period.

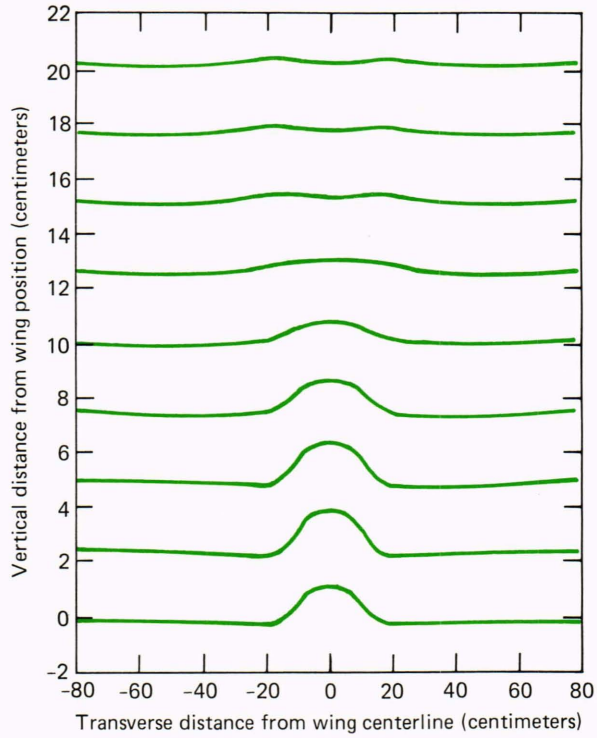

Figure 2—FISHBONE predictions of displacements for constant N case; t = 0.5 BV period.

only internal waves are generated. However, the equations used to calculate the flow were the full set with the nonlinear terms retained. The results show that these terms are indeed insignificant for this case.

The measurement resolution of 1 centimeter would have taxed the storage and speed of the computer doing the numerical computations, so the grid chosen to calculate the flow had grid points placed every 2.54 centimeters. Thus, when the data are presented, the experimental results are interpolated onto the computational grid.

It must be borne in mind that all the calculations to be presented result from an inviscid treatment of the problem. No viscous or turbulent phenomena have been considered. Regions where those phenomena may be important, such as the turbulent wake of the wing, will show the limitations of the present approach.

Figure 2 shows the computational results, in raster plot form, for the first APL experiment with a constant background stratification. The figure corresponds to 0.5 ($2\pi/N$), a time equal to one-half of a Brunt-Väisälä period. In order to compare the experiment and the prediction, the experimental values of Fig. 1 are interpolated onto the same points of Fig. 2; they both are shown in Fig. 3.

The zero point on the abscissa is the middle point on the wing; the zero of the ordinate is the nominal vertical position of the wing in the tank. The agreement at this early point in the development is not bad. Surprisingly, the levels and phase of the disturbance are correct, even in the turbulent wake region near the wing. Far above the wing, the agreement is also good, but, although earlier calculations show that the displacement levels are decreasing in the intermediate region, the agreement there is not good.

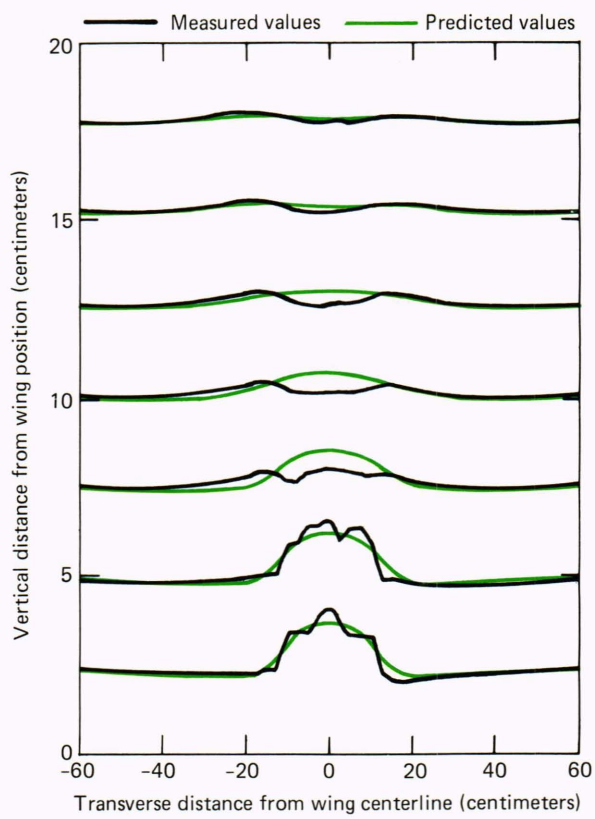

Figure 3—Comparison of FISHBONE predictions and measured displacements; constant N, t = 0.5 BV period.

That disagreement is obviously due to some initial transient related to starting the calculation and/or the experiment, because the comparisons at 1.0, 1.5, and 2.0 Brunt-Väisälä periods are quite good for the far field waves. They are shown in Figs. 4 through 6. All the figures show excellent agreement in both amplitude and phase. Note in Fig. 6, the latest time shown, the residual of the turbulent wake and its alteration of the smooth wave pattern. Although it is difficult to distinguish in these plots, the calculations are always symmetric since no way was input to deviate from symmetry, whereas the experimental results are asymmetric even away from the turbulent region.

Another way to view the data is to plot contours of constant nondimensional density perturbation in the *y-z* plane of the vortex. This could be done with either computed or experimental data, but only the computed data will be displayed here. This type of plot serves a very useful purpose in subsequent discussions. Figures 7 and 8 show the density contours in the right-half plane of the entire computational domain, at times equal to periods of 0.5 and 1.0 Brunt-Väisälä. Nothing extraordinary can be observed. Note that at the right side boundary a small disturbance can be seen in the center of the field. But in general, the assumption of no disturbance at the computational boundary is reasonably valid and can be expected to be so, probably at least until 2.0 Brunt-Väisälä periods are reached; hence the good comparisons of Figs. 4 through 6.

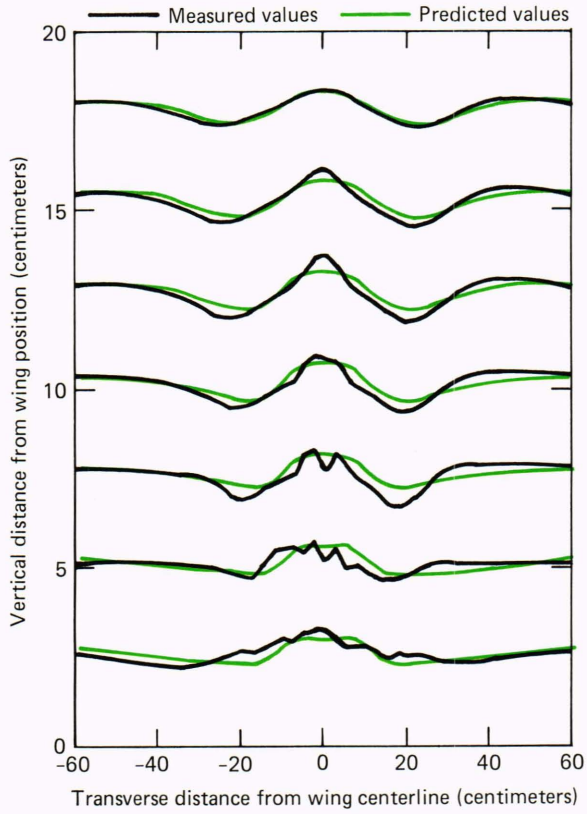

Figure 5—Comparison of FISHBONE predictions and measured displacements, constant N, t = 1.5 BV periods.

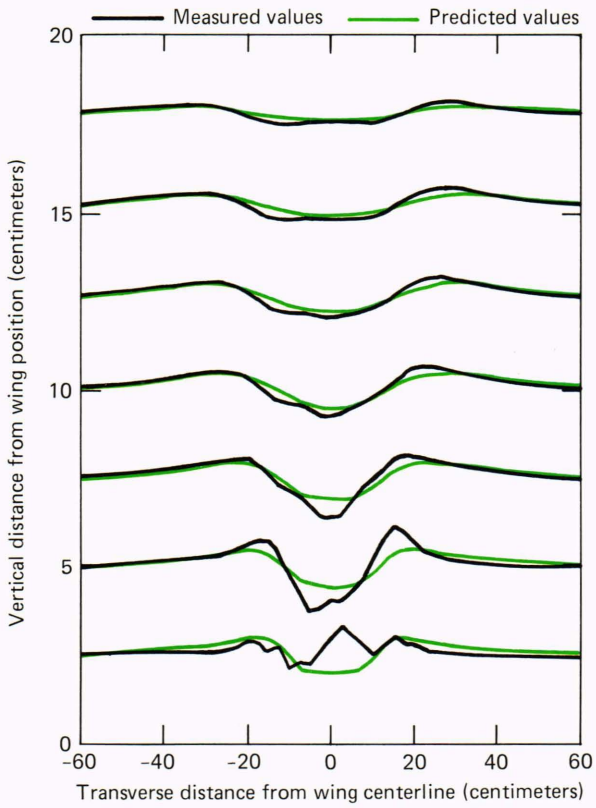

Figure 4—Comparison of FISHBONE predictions and measured displacement; constant N, t = 1.0 BV period.

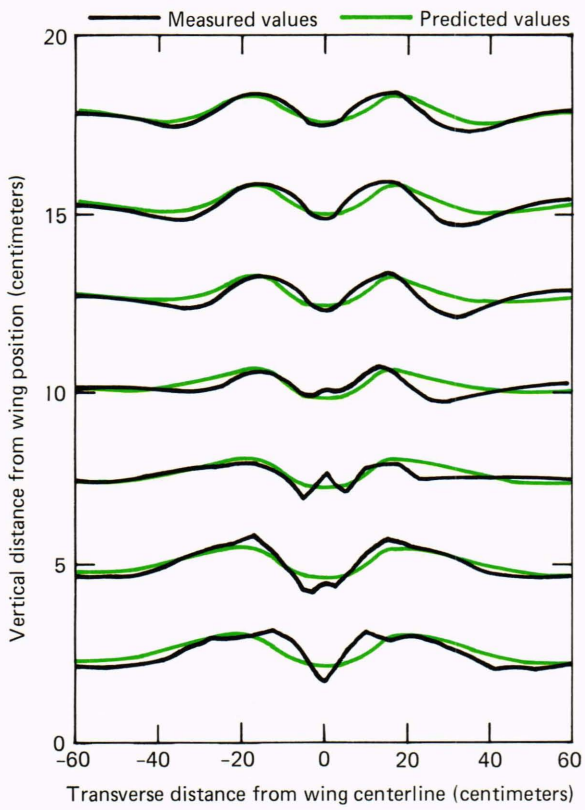

Figure 6—Comparison of FISHBONE predictions and measured displacements; constant N, t = 2.0 BV periods.

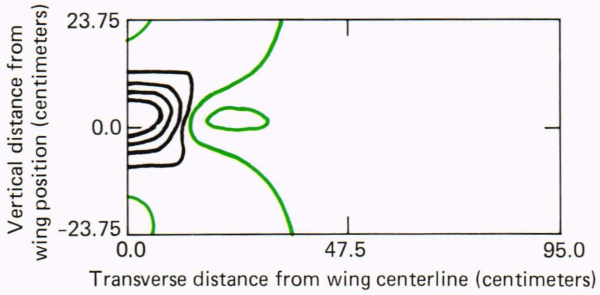

Figure 7—Density perturbation contours; constant N, t = 0.5 BV period.

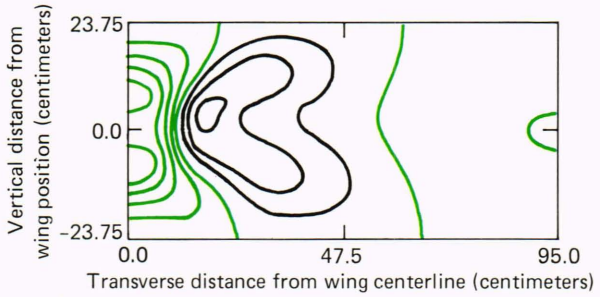

Figure 8—Density perturbation contours; constant N, t = 1.0 BV period.

The towing tank was stratified for the second series of tests with the variable Brunt-Väisälä profile shown in Fig. 9. The corresponding profile used in the numerical calculations is shown in Fig. 10. This type of profile corresponds to what is called an oceanic duct. Waves propagating within such a stratified background can be trapped in the peak N region, similar to the properties of a waveguide. The computational results that follow will bear this out. For this variable Brunt-Väisälä profile case, the reference value of N is taken to be N at the wing location (z = 0), again giving an F_V value of approximately 1/35.

Figure 11 shows the raster plot comparison of displacement produced by FISHBONE and the laboratory experiment at 1.0 Brunt-Väisälä period. Except for the region $z < 7.5$ centimeters affected by the turbulent wake, where the phase is still good, the comparison is very good. The calculations even reproduce the node in the displacement between z = 12.5 and 15.0 that is not present in the comparable time raster plot for the constant N case (Fig. 3). However, later ($\approx$2.0 Brunt-Väisälä periods), the phase comparisons are very poor because of the ducting phenomenon described above. The contour plots for the variable N case depict the ducting very clearly. Figures 12 and 13 show the contours of density perturbation for the variable N case for 0.5 and 1.0 Brunt-Väisälä periods; the center of the duct is at z = 17.5. Even for the 0.5 Brunt-Väisälä period time, there is a noticeable perturbation propagating to the right. At 1.0 Brunt-Väisälä period (Fig. 13), a perturbation has reached the boundary and is being followed by a significant wave. The figures depict very graphically what is meant

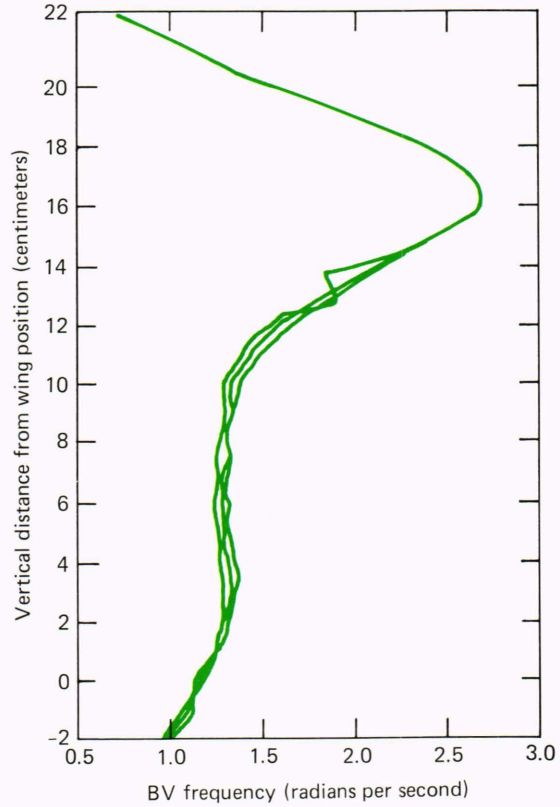

Figure 9—Experimental stratification for the variable BV case (data from three runs).

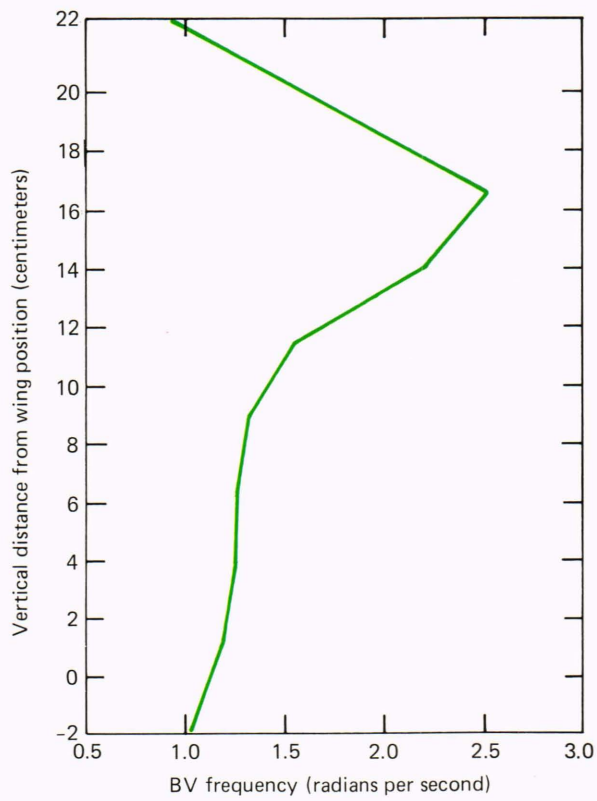

Figure 10—Stratification used in numerical predictions of the variable BV case.

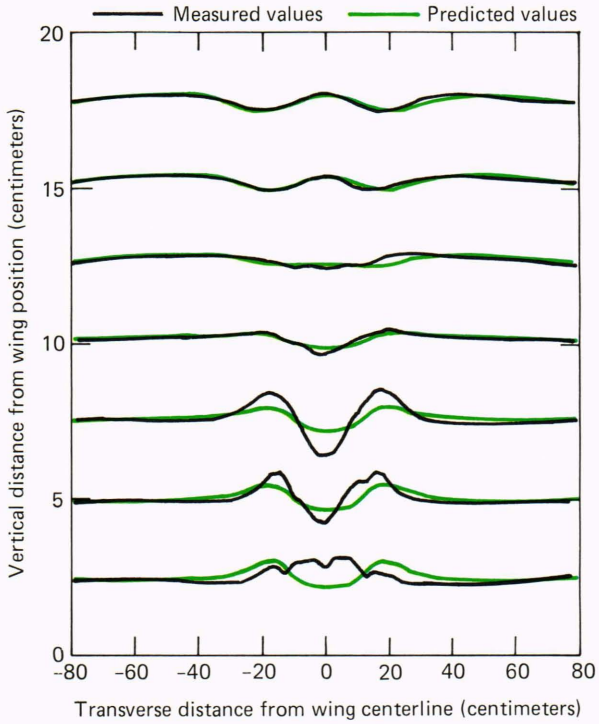

Figure 11—Comparison of FISHBONE predictions and measured displacements; variable N, t = 1.0 BV period.

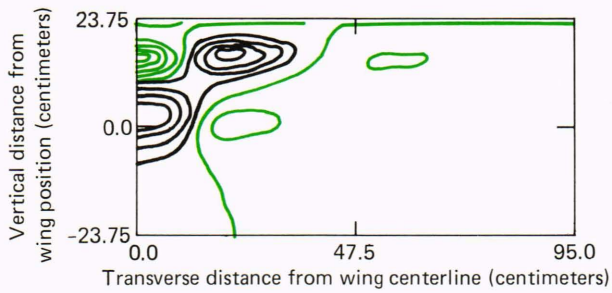

Figure 12—Density perturbation contours; variable N, t = 0.5 BV period.

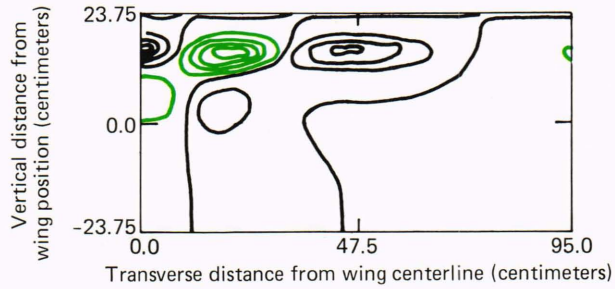

Figure 13—Density perturbation contours; variable N, t = 1.0 BV period.

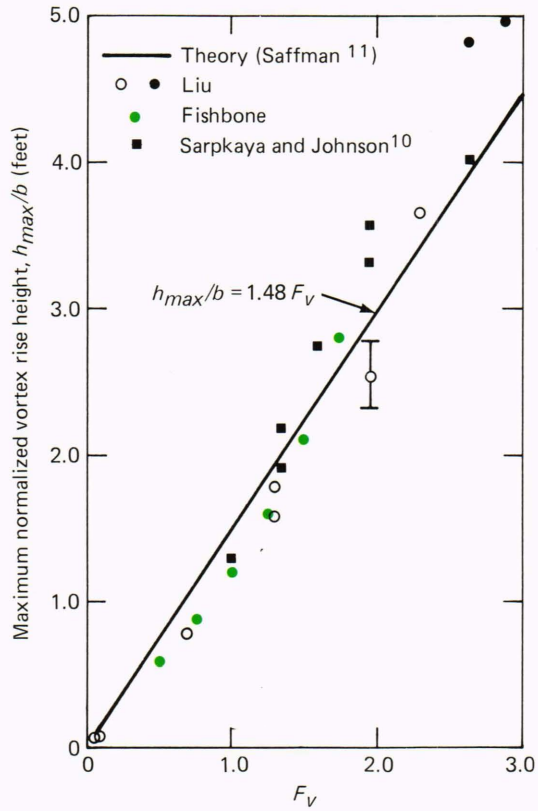

Figure 14—Maximum rise height of vortex pairs.

by ducting of the internal waves. By the time 2.0 Brunt-Väisälä periods are reached, the boundary condition of no perturbation has been badly violated, and wave reflections have taken place that destroy the good agreement found for the constant N case.

Neither of these cases experienced any motion of the initial vortex pair because F_V was quite small. Other experiments and an old theoretical prediction allow the nonlinear aspects of the FISHBONE code to be evaluated. When a vortex moves in a stratified fluid, the presence of the stratification acts as a retarding force on the motion of the vortex. There is a transfer of energy between the kinetic energy of the vortex and the potential energy of the density perturbations. After some time, depending on the F_V, the vortex reaches a maximum distance away from its initial position and then reverses direction and falls back toward its starting position. As in the previous cases, the controlling parameter is F_V; for different values of F_V, the rise height of the maximum vortex varies.

A theory of Saffman[11] models the physics of the process and, without solving the exact Eqs. 6 and 7, predicts a linear relationship between rise height and F_V. The experiments of Liu[9] and of Sarpkaya and Johnson[10] measure the vertical position of vortices produced in a manner similar to the APL experiments and yield the data shown in Fig. 14. This behavior was also modeled with the FISHBONE code by inputting wing velocities calculated to give specific values of F_V in the range 0.5 to 1.75. The position of the maximum value of vorticity was tracked, and the farthest excursion from its initial point was taken to be the maximum vortex rise height. The predicted values are also plotted on Fig. 14, normalized by the initial vortex separation distance, b.

It can be seen in the figure that the linear relationship between rise height and F_V predicted by Saffman is confirmed, at least for $F_V \leq 1.0$. The constant of proportionality given by Saffman, based on the assumptions he made, is too large, but obviously the physical reasoning is sound. The experiments and the FISHBONE predictions agree very well for the low range of F_V, giving a proportionality constant of 1.20. This indicates that for these lower energy vortices the retardation of the motion is strictly an inviscid process because FISHBONE is inviscid, and the energy is simply being transferred from the vortex to the density perturbations. However, as F_V increases, the FISHBONE results deviate above both the linear relationship and the experiments, implying the need for some dissipative mechanism like turbulence. The actual numerical calculations also show a tendency for the energy to be deposited increasingly in smaller scales, another sign that a dissipative process is required to remove the energy. Were there an energy-absorbing mechanism in the code, the motion would not be as vigorous, and the predicted rise height would approach the experimental results for the "higher" Froude numbers.

CONCLUSIONS

The consequences of stratification on the classical inviscid fluid dynamics problem of motion of a pair of counterrotating vortices have been discussed in the context of explaining the capabilities and limitations of numerical predictions. More complications would result from the inclusion of more physics such as a turbulence model for the vortex rise problem or proper boundary conditions that let the propagating disturbance pass out of the restricted computational domain used for the ducted propagation problem. In spite of the relative simplicity of the inviscid approach, it has been shown that within the range of validity of the equations chosen to represent the physics and of the numerical procedures used to solve the equations, excellent agreement with experimental results and insights into the physical mechanisms can be obtained.

REFERENCES

[1] J. T. Lin and Y. H. Pao, "Wakes in Stratified Fluids," *Ann. Rev. Fluid Mech.* **11**, 317-338 (1979).

[2] S. Hassid, "Collapse of Turbulent Wakes in Stably Stratified Media," *J. Hydrol.* **14**, 25-32 (1980).

[3] H. E. Gilreath and A. Brandt, "Experiments on the Generation of Internal Waves in a Stratified Fluid," AIAA 16th Fluid and Plasma Dynamics Conf., AIAA Paper No. 83-1704 (1983).

[4] R. S. Hirsh and J. H. Stuhmiller, *Turbulence Generated Internal Waves,* JAYCOR Final Report (Apr 1979).

[5] R. W. Metcalfe and J. J. Riley, "Numerical Simulations of Density Stratified Turbulence," 8th National Congress of Applied Mechanics (1978).

[6] R. S. Hirsh, T. D. Taylor, M. M. Nadworny, and J. L. Kerr, "Techniques for Efficient Implementation of Pseudo-Spectral Methods and Comparisons with Finite Difference Solutions of the Navier-Stokes Equations," in *Lecture Notes in Physics* **170**, Springer-Verlag, pp. 245-251 (1982).

[7] B. Thwaites, *Incompressible Aerodynamics,* Clarendon Press, Oxford (1960).

[8] A. Brandt and D. A. Hurdis, "Simulation of Oceanographic Processes in the Hydrodynamics Research Laboratory," *Johns Hopkins APL Tech. Dig.* **3**, 42-48 (1982).

[9] H. T. Liu, private communication (1981).

[10] T. Sarpkaya and S. K. Johnson, *Trailing Vortices in Stratified Fluids,* Naval Postgraduate School Report NPS-69-82-003 (1982).

[11] P. G. Saffman, "The Motion of a Vortex Pair in a Stratified Atmosphere," *Stud. Appl. Math.* **II**, 107-119 (1972).

ACKNOWLEDGMENT—I would like to acknowledge the cooperation of David A. Hurdis in providing unpublished results of his experimental investigation.

THE AUTHOR

RICHARD S. HIRSH was born in New York City in 1942. He received his Ph.D. in fluid mechanics from the Case Western Reserve University in 1970. While at NASA's Langley Research Center, he switched his area of specialization to the then-emerging field of computational fluid dynamics. After working at Douglas Aircraft Company, he joined APL in 1980 and is in the Hydrodynamics Group of the Submarine Technology Department, where he has been involved in the review and improvement of many hydrodynamic simulation codes. He was also on the supercomputer technical panel. In addition, he continued research in computational fluid dynamics, concentrating on the use and implementation of pseudospectral methods.
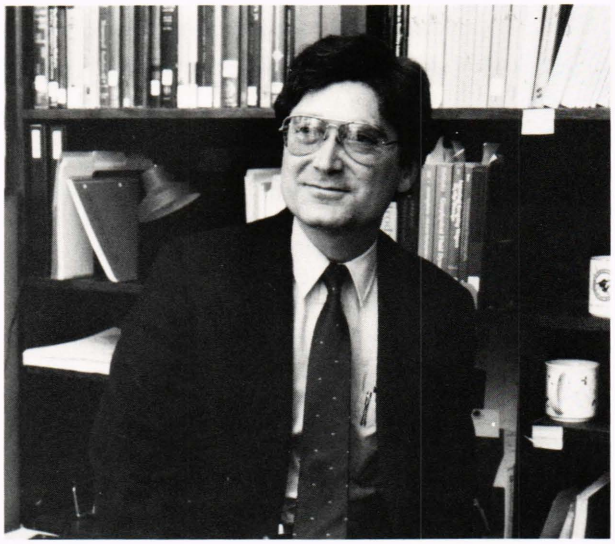
Dr. Hirsh has participated in each International Conference on Numerical Methods in Fluid Dynamics since 1974 and is an associate reviewer of papers for the meetings as well as being a reviewer for three other major computational journals. In 1983, he was invited to give a series of lectures on numerical methods at the Von Karman Institute for Fluid Dynamics in Brussels. He has been invited to spend two weeks during the summer of 1985 at the Institute for Computer Applications in Science and Engineering at NASA/Langley.